11

Application of siRNA Against SARS in the Rhesus Macaque Model

Qingquan Tang, Baojian Li, Martin Woodle, and Patrick Y. Lu

Summary

Containment of the SARS coronavirus (SCV) outbreak was accompanied by the rapid characterization of this new pathogen's genome sequence in 2003, encouraging the development of anti-SCV therapeutics using short interfering RNA (siRNA) inhibitors. A pair of siRNA duplexes identified as potent SCV inhibitors *in vitro* was evaluated for *in vivo* efficacy and safety in a rhesus macaque SARS model using intranasal administration with clinical viable delivery carrier in three dosing regimens. Observations of SCV-induced SARS-like symptoms, measurements of SCV RNA presence in the respiratory tract, microscopic inspections of lung histopathology, and immunohistochemistry sections from 21 tested macaques consistently demonstrated siRNA-mediated anti-SCV activity. The prophylactic and therapeutic efficacies resulted in relief of animals from SCV infection-induced fever, diminished SCV in upper airway and lung alveoli, and milder acute diffuse alveoli damage (DAD). The dosages of siRNA used, 10 to 40 mg/kg, did not show any sign of siRNA-induced toxicity. These results support that a clinical investigation of this anti-SARS siRNA therapeutic agent is warranted. The study also illustrates the capability of siRNA to enable a massive reduction in development time for novel targeted therapeutic agents. We detail a representative example of large-mammal siRNA use.

Key Words: RNA interference (RNAi); small interfering RNA (siRNA); severe acute respiratory syndrome (SARS); SARS coronavirus (SCV); diffuse alveoli damage (DAD); proinflammatory cytokines.

1. Introduction

The outbreak of severe acute respiratory syndrome (SARS) posed an urgent need to understand disease pathogenesis ***(1–3)*** and biology of the causative agent, now identified as SARS coronavirus (SCV) ***(4–8)***. SARS patients usually

From: *Methods in Molecular Biology, vol. 442: RNAi: Design and Application*
Edited by: S. Barik © Humana Press, Totowa, NJ

develop a high fever followed by severe clinical symptoms including acute respiratory distress syndrome (ARDS) with diffuse alveolar damage (DAD) at autopsy ***(2,4,9)***. The containment of SARS was achieved largely through traditional quarantine and sanitation measures ***(9,10)***. Since SARS is a newly emerging disease and the first coronavirus-mediated disease, a safe and effective vaccine was not available, nor was an established anti-coronavirus therapeutic ***(11)***. Candidate vaccines became possible only once the causative virus was identified; efforts already have advanced to monkey models and clinical testing, spanning many approaches from attenuated and modified vaccinia virus, MVA ***(12)***, recombinant parainfluenza virus, BHPIV3 ***(13)***, inactivated whole virus ***(11)***, to DNA vaccines ***(14)***. However, these rapid advances require rigorous and lengthy studies ***(15)***, illustrating the difficulty in using vaccine development to offer rapid solutions for new emerging infectious diseases. To treat SARS patients, combinations of existing drugs have been developed including ribavirin, antibiotics, anti-inflammatory steroids, and immune stimulators, and this approach had achieved some clinical successes ***(16–21)***. Many ongoing efforts to develop SARS-specific drugs such as screening of small molecule inhibitors and current biological approaches will clarify the strengths and weaknesses of each approach, based on the ultimate success rate, and the time and cost incurred.

The identification of SCV as the causative pathogen of SARS was critical for containment and patient management. This was achieved mainly by demonstration that exposure of cynomolgus macaques to SCV resulted in similar symptoms to those of SARS patients ***(1,2)*** while also creating the first animal disease model critical not only for understanding SARS pathogenesis but also for evaluating potential vaccines and novel therapeutics ***(13)*** and was followed by the development of several others ***(12,14,17,22)***.

Demonstration of protection by PEGylated interferon-α from SCV infection in cynomolgus macaques, as seen in SARS patients, gives further proof of the effectiveness of such model ***(21)***. Recently, a rhesus macaque model for SARS has been established with intranasal instillation of SCV strain PUMC01, showing many elements of pathology similar to those of SARS patients and the cynomologus macaque model (*see* **Notes 1–3**). The pathogeneses include elevated body temperature, low appetite, and acute DAD clearly visible at 7 days' post-infection (d.p.i.), but with somewhat worse severity ***(23–26)***. Thus, it offers an ideal model for evaluation of therapeutic candidates inhibiting SCV specifically as potential treatments for SARS.

The search for developing antiviral agents directly from viral genome sequences has led to thorough investigations of siRNA ***(27,28)***. We previously screened 48 siRNA candidates targeting elements throughout the entire SCV genome and identified several active siRNA duplexes using fatal rhesus

monkey kidney (FRhK-4) cells ***(29)***. Other active siRNA sequences inhibiting SCV have also been reported from screening only a handful of candidate open reading frames in cell culture with either synthetic siRNA ***(30–32)*** or plasmid-expressed shRNA ***(33)***. Translation from *in vitro* inhibition to efficacious use to treat clinical respiratory infections depends on clinically acceptable and effective administration. A pair of siRNAs showing prominent prophylactic and therapeutic activities in the cell culture study ***(29)***, referred to as siSC2 and siSC5, were further evaluated *in vivo*, first in mice using a reporter gene assay and subsequently using a clinically acceptable intranasal administration in the recently established rhesus macaque SARS model ***(23–26)***. The study revealed strong evidence that these siRNA duplexes are potent prophylactic and therapeutic anti-SARS agents, and there is a lack of toxicity in the non-human primate model. These results further support the growing expectation that siRNA can fulfill the need for moving rapidly from gene sequence to selective inhibitory agents, and for many previously intractable therapeutic targets (*see* **Notes 4 and 5**).

2. Materials

1. The SCV strain for study. We started with PUMC-01 (AY350750), isolated from a patient in the Peking Union Medical Hospital (PUMH) and propagated in cultured Vero cells. A titer of 10^5 TCID50/1.0 mL is needed.
2. FRhk-4 cells for studies of SCV infection and siRNA effect.
3. The rhesus macaque (*Macaca mulatta*) of appropriate number. This animal model was developed using intranasal inoculation of PUMC01 SCV ***(23–25)***. All monkeys are three years old with an average body weight of 3 kg and confirmed as SARS-antibody negative before SCV challenge using a standard SARS-specific ELISA assay ***(23–25)***.
4. Bio-safety level 3 (BSL-3) facility for the virus and infected animals.
5. Synthetic siRNA (see amounts later).
6. Carriers: D5W (5% glucose in sterile water); Infasurf™ (Forest Labs, St. Louis, MO).
7. Standard vivarium and approved monkey colony.
8. Reagents for viral growth and assay.
9. Standard procedures and reagents for the isolation of nucleic acids and for RT-PCR.
10. Tools for phlebotomy.
11. Assays for liver enzymes.
12. ELISA diagnostic kits for detection of anti-SCV IgG or IgM (Hau Da Biotech, Beijing, China) used according to the manufacturer's protocol.
13. Procedure and reagents for microscopic inspections of lung histopathology that also requires an investigator experienced in this area (see Section 3).

14. The secondary antibody for the detection of SCV and monoclonal antibodies to monkey CD4, CD8, CD35, CD38, CD68 and Keratin were all purchased from Zhongshan Biotechnology Co., Ltd. (Beijing, China).

3. Methods

We offer representative examples of our procedures and the corresponding results. We expect that readers will test their own targets and optimize the protocol accordingly.

3.1. Selection of siRNA Duplexes

1. Two SCV-specific siRNA duplexes, siSC2 and siSC5, targeting, respectively, the SCV genome at spike protein and ORF1b (nsp12) coding regions, were designed based on SCV complete genome sequence (NC-004718), derived from strain TOR-2 (AY274119).
2. Selection of siSC2 and siSC5 was based on their anti-SARS potencies validated in the cell culture study ***(29)***; they were always used as a mixture (siSC2-5) of equal amounts.
3. A pair of control siRNA duplexes, siCONa and siCONb, without any homology to human and SARS genomes, were also used in the mixture (siCONa-b). Another pair of unrelated control siRNA duplexes, siCONc and siCONd, were used in the mixture in the mouse study (siCONc-d).
4. All siRNA duplexes consist of two complementary 21-nt RNA strands with 3′ dTdT-overhangs and were manufactured by Qiagen (Gaithersburg, MD):

```
siSC2: 5′-GCUCCUAAUUACACUCAACdtdt-3′
  3′-dtdtCGAGGAUUAAUGUGAGUUG-5′
siSC5: 5′-GGAUGAGGAAGGCAAUUUAdtdt-3′
  3′-dtdtCCUACUCCUUCCGUUAAAU-5′
siCONa: 5′-CCGCUGGAGAGCAACUGCAdtdt-3′
  3′-dtdtGGCGUCCUCUCGUUGACGU-5′
siCONb: 5′-GCUAUGAAACGAUAUGGGCdtdt-3′
  3′-dtdtCGAUACUUUGCUAUACCCG-5′
siCONc: 5′-GCUGACCCUGAAGUUCAUCdtdt-3′
  3′-dtdtCGACUGGGACUUCAAGUAG-5′
siCONd: 5′-GCAGCACGACUUCUUCAAGdtdt-3′
 3′-dtdtCGUCGUGCUGAAGAAGUUC-5′
```

3.2. Electron Microscopy

1. Infect FRhk-4 cells by SCV, with or without treatment of siSC2-5, harvest and fix in 2.5% glutaraldehyde (Electron Microscopy Sciences, Fort Washington, PA) for 4 h and postfix in 1% osmium tetroxide for 1 h.

2. Transfer the cells to a 1.5-mL tube and centrifuge at 1,000 rpm for 10 min.
3. Remove the supernatant and add a liquidized 2% agarose (Sigma, St. Louis, MO) solution at 55–60 °C to the cell pellet. After the gel solidifies, prepare approximately 1-mm^3 cubes containing cell pellet and dehydrate in graded ethanol.
4. Embed the cubes in epoxy resin (Polysciences, Warrington, RI). Prepare ultra-thin sections (70 nm thick) and stain with uranyl acetate (Electron Microscopy Sciences) and lead citrate (Leica Microsystems, Vienna, Austria).
5. Examine the sections under a Philips EM208S electron microscope at 80 kV. Mark the images with a 200-nm-long scale bar.

3.3. Delivery of Nucleic Acid into Mouse Lungs

For cost-saving purposes and to minimize handling of the pathogenic SCV, the mouse is first used to screen a large number of siRNAs against recombinant SCV targets before moving to the monkey.

1. Divide 20 BALB/c mice (6–8 weeks old) into four groups ($N = 5$).
2. The pCI-scLuc reporter plasmid was constructed earlier by inserting a DNA fragment containing siSC2 and siSC5 targeted sequence DNA between its CMV-driven transcriptional initiation site and luciferase coding sequence.
3. Two carrier solutions, D5W and Infasurf™ (*see* **Note 6**), were used for intratracheal deliveries of the siSC2-5, siCONc-d, and pCI-scLuc plasmids.
4. Mix 30 μg of pCI-scLuc and an equal amount of corresponding siRNA (*see* **Note 7**) with 100 μL of carrier solution and administer intranasally into the mouse lungs (*see* **Note 3** in Chapter 6).
5. At 24 h post-delivery, sacrifice the mice and harvest the lung tissues. Homogenize in 800 μL of 1X Reporter Lysis buffer (Promega,) using Lysing Matrix D (Bio 101 System, CA) in a FastPrep-FP120 (Bio 101 System) at speed 4.0 for 40 sec.
6. Centrifuge at 12,000 rpm for 2 min at 4 °C. Use 10 μL of supernatant for measurement of luciferase activity using a Luciferase Assay kit (Promega) and a luminometer (Analytical Luminescence Lab, TN) following manufacturer's protocol.

3.4. SCV Infection in the Rhesus Macaque Model

A typical example of study design is shown in **Table 1** (*see* **Notes 8–12**).

1. Inoculate SCV-negative healthy monkeys with PUMC01 at 10^5 TCID50/1.0 mL through nasal instillation, mimicking the natural route of SCV infection of SARS patients.
2. Also deliver 30 μg of siSC2-5 and siCONa-b siRNA agents in 3 mL of D5W intranasally.
3. After the macaques are SCV-challenged and treated with siSC2-5 or siCONa-b, observe for clinical signs daily, including body temperature, size of lymph nodes, body weight, coughing, sneezing, appetite, aggressiveness, etc.

Table 1
Sample Study Design and Dosing Regimen

Groups		Viral Infection Control (IC)	Nonspecific Sequence Control (NS)	Prophylactic Treatment (PL)	Co-delivery Treatment (CD)	Postexposure Treatment (PE)
Cohort ($n = 4$)		007, 205, 206, 212	163, 167, 202, 208	130, 138, 151, 203	002, 021, 077, 166	210, 015, 214, 023
Sex		M/M/F/F	M/M/F/F	F/F/M/M	F/M/M/F	F/M/M/F
Ages (year)		3	3	3	3	3
Body weight (kg)		3.43 ± 0.37	3.60 ± 0.29	3.41 ± 0.23	3.71 ± 0.35	3.19 ± 0.58
Viral dosage (1 mL)		10^5 $TCID_{50}$	$10^5 TCID_{50}$	$10^5 TCID_{50}$	$10^5 TCID_{50}$	$10^5 TCID_{50}$
siSC2-5				30 mg/3 mL/dose	30 mg/3 mL/dose	30 mg/3 mL/dose
siCONa-b			30 mg/3 mL/dose			
Dosing regimen	−4 h			√		
	Co-delivery		√		√	
	4 h					√
	24 h		√		√	√
	72 h		√		√	√
	120 h		√		√	
Total dosage			120 mg/120 hr	30 mg/120 hr	120 mg/120 hr	90 mg/120 hr
Termination @	Day 7:	205, 206	167, 202	138, 151	002, 077, 166	015, 210
	Day 20:	007, 212	163, 208	130, 203	021	023, 214

Twenty rhesus monkeys belonging to five test groups were used in the study with same viral titer challenge but different drug dosing regiments of siRNA. Four monkeys were tested in each group and necropsied at either 7 or 20 d.p.i. in BL-3 environment. One additional monkey was used as no-viral-infection control, and the lung tissue was collected for the histology analysis.

4. At 4 d.p.i., take oropharyngeal swabs from the SCV-challenged monkey and estimate virus by the RT-PCR of genomic RNA and reisolation.
5. Collect blood samples on 4, 7, 10 and 19 d.p.i. for routine laboratory examination including liver enzymatic analysis and the SARS-specific antibody detection as detailed below.
6. For liver enzymatic analysis, we chose alanine aminotransferase (ALT), lactic acid dehydrogenase (LDH), creatine kinase (CK), and aspartate aminotransferase (AST) at 7 d.p.i. after the SCV infection of all 20 animals from every tested group. Their levels should all increase. In our experiments, routine blood examination also indicated a marked increase of hemoglobin (HGB) and platelets (PLT) in SCV-infected macaque, which is contradictory to another report on the macaque SARS model ***(22)*** and reports on SARS patient ***(9,10,16)***.
7. Detect anti-SCV IgG or IgM by standard ELISA.
8. When the macaques are necropsied at 7 and 20 d.p.i., collect lungs and conduct thorough microscopic inspections of lung histopathology.
9. Collect other organs as needed with appearance and morphology inspections and further compare using an internal organ coefficient of each group, based on wet weight of organ per 100 g of average body weight.

3.5. RT-PCR and SCV Reisolation

1. Isolate total cellular RNA using a QIAamp RNA isolation kit (Qiagen). Synthesize the first strand of cDNA using RNAse H^+reverse transcriptase and random primers (Invitrogen), according to manufacturer's protocol. The forward and reverse primers and the fluorescence probe used for PCR were 5′-GCATGAAATTGCCTGGTTCAC-3′, 5′-GCATTCCCCTTTGAAAGTGTC-3′, and FAMAGCTACGAGCACCAGACACCCTTCGAAATRMA, respectively.
2. Perform real-time PCR using ABI7900 Sequence Detection System (ABI, CT) and all PCR in triplicates.
3. Perform SCV reisolation using the swab samples by serial passage on Vero cell culture as previously described ***(24,25)***.

3.6. Lung Histopathology and Immunohistochemistry Analyses

1. Create epoxy resin-filled lung blocks from the right upper and right middle lobes and perform routine pathology analysis. Briefly, first fix the tissues with 10% formaldehyde, embed in resin, section, stain with H&E or silver stain, and then subject to microscopic examination.
2. The severity of lung damage is determined based on observations of five different sections of each lung by readouts from three independent pathologists with blind sample IDs.
3. Resin-embedded tissue sections are "de-waxed" and rehydrated for the immunohistochemistry analysis as follows. Incubate the tissue sections in 0.3% hydrogen peroxide for 30 min and rinse with PBS. Then treat with normal sera in humid

chamber for 20 min, and treat with a 1:100 diluted primary antibody followed by a treatment with appropriate 1:1,000 diluted secondary antibody.
4. After substrate staining and hematoxylin counterstaining, examine the slides under microscope. Our first antibody was the convalescent antisera from a SARS patient of PUMH (STS-D, Zhang-03), and the second antibody was a biotinylated goat–anti-human IgG (PK-4001, ABC kit).
5. Identify the cell types based on the separate staining with corresponding mAbs using methods described previously ***(24,25)***.
6. The SCV-infected cell counts within each microscopic image from every lung tissue section are independently collected by three readouts with blind sample IDs. Average cell counts of four lungs from each group ($N = 4$) are compared.

3.7. Statistical Analysis

1. We analyzed data using the Student *t*-test for Luciferase expression in mouse lungs (**Fig. 1d**), mean body temperature (**Fig. 4a**), histopathology score comparison (**Fig. 4d**), and SCV-infected cell counts (**Fig. 5h**).
2. Statistical significance is only considered when $P < 0.05$. The regression analysis is conducted based on the average body temperature of each group at each day point (**Fig. 4b**).

4. Notes

(Abbreviations: IC = viral infection control; NS = nonspecific siRNA control; PL = prophylactic treatment; CD = co-delivery treatment; and PE = postexposure treatment.)

1. While concern remains whether the macaque SARS models have good clinical relevance ***(15,22–26)***, the rhesus macaque model in the present study using a highly virulent SCV strain PUMC01 simulates the pathogenesis process in SARS patients ***(9,10,39)***. Clear clinical relevance of this model is found in most of the parameters studied including elevated body temperature, lung pathology, and SCV antigen detection in epithelial originated type I pneumocytes, type II pneumocytes, and macrophages, providing strong support that the model has the attributes required for evaluation of anti-SCV siRNA.
2. In this study the siSC2-5 was dosed through the same intranasal route as the SCV challenge, with prophylactic, concurrent, or early postexposure treatments within a period of 5 d.p.i. All three different treatment regimens achieved potent suppression of SCV-induced SARS pathogenesis. Detection of the SCV RNA genome with RT-PCR revealed that only 25% of oropharyngeal swab samples from the treated group were positive versus all samples from the control groups being positive. Similarly, using immunohistochemistry detection, SCV-infected cell counts significantly decreased in the lung sections from the treated groups. Along with the reduced viral spread was a substantial reduction in the SARS-like clinical symptoms and the lung histopathology.

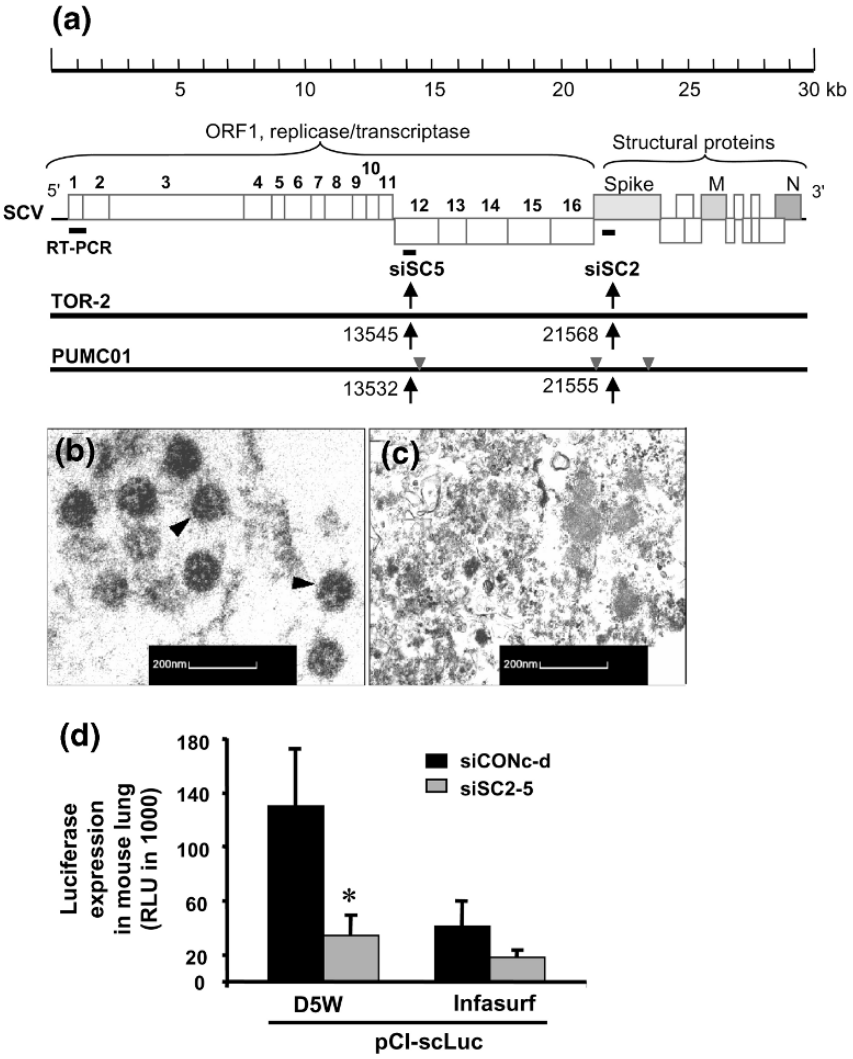

Fig. 1. Selection and validation of siRNA duplexes targeting SCV sequence. (a) The RT-PCR amplified region is marked at the most upstream of open reading frame 1 (ORF1). Two siRNA duplexes, siSC2 and siSC5, target the coding regions of Spike and NSP12 of the SCV genome, respectively. Black arrows indicate the locations of the two targeted sequences within the viral RNA genome. (b) EM image of SCV particles indicated by arrows within SCV infected FRhK-4 cell. (c) EM image of the SCV infected FRhK-4 cell with postexposure treatment using siSC2-5 combination. (d) Luciferase expression in mouse lungs after codelivery of the expression plasmid pCI-scLuc and either the specific siSC2-5 or the nonspecific siCONc-d control, in either D5W solution or Infasurf™ solution. * indicates $P < 0.05$, $N = 5$.

3. A few comments regarding the mechanism of siRNA action against SCV are in order. The present study is designed to investigate the siRNA-mediated anti-SCV effects in both the upper airway and deep lung of SCV-exposed macaques that occurred during the early phase of the viral infection and disease progression. The impact of the siSC2-5 on the early phase of SCV infection is first exhibited in the mucosal epithelial cells of the upper respiratory tract, expected since siSC2-5 and SCV are both administered through intranasal instillation and all siRNA dosings are completed within the first 5 days. This siSC2-5 anti-SARS efficacy can result from one or more of the following three possible mechanisms: protection of cells from a successful SCV infection; degradation of SCV mRNA inhibiting viral protein synthesis in infected cells ***(29)***; or obstruction of SCV genome replication and spread to uninfected cells. Here a single prophylactic dose of siSC2-5 provides protection comparable to therapeutic treatment using multiple doses. Similar clinical benefits were observed from both treatment regimens of CD and PE, indicating that researchers may try to improve dosages and regimens. These studies with an early siRNA intervention in SCV exposure resulted in a long-lasting inhibitory effects on the average body temperature, viral infected cell counts, and lung damage for 20 days. Considering that SARS-specific neutralizing antibody in SCV-infected macaques can be detected as early as 10 d.p.i., we speculated that the clinical benefit of siRNA-mediated anti-SARS activity observed in this study is the consequence of combined activities from the siRNA agent and the neutralizing antibody, suggesting that multiple antiviral mechanisms were operative (also *see* **Note 12**).
4. There are interesting advantages to using siRNA in SARS ***(29,34)***. The release of proinflammatory cytokines from the alveolar macrophage has been proposed to play a prominent role in SARS pathogenesis and as a point for intervention ***(9)***. In addition, the presences of hemophagocytosis ***(54,55)*** or an interferon-γ-related cytokine storm in SARS patients ***(56)*** complicates our understanding of SARS pathogenesis but also argues against the use of interferon therapy in clinical treatment, despite studies in the cell culture ***(18–20)***, a macaque model ***(21,41)***, and SARS patient ***(57)***, showing inhibition of SCV with interferon treatment. In contrast to such proinflammatory cytokine treatments, intranasal delivery of siRNA offers a unique compliment of high-specificity inhibition of the target SCV with minimal induction of a proinflammatory cytokine antiviral response that may help to avoid exacerbating symptoms and lung damage. Reports of siRNA administration in mouse models for lung delivery have evaluated different formulations including cationic polymer and lipid complexes using either intravenous or airway administration ***(34–37)*** and shown efficient anti-RSV and anti-influenza effects as well (e.g., *see* **Chapter 6**).
5. Selection of potent SCV-specific siRNA agents: Two siRNA duplexes, siSC2 and siSC5, targeting the SCV genome at spike protein coding and ORF1b (nsp12) regions, respectively, were chosen for *in vivo* studies for the following reasons: (a) The targeted sequences of these two siRNA duplexes exhibit a 100% homology to the strain TOR-2 used in the cell culture study ***(29)***, to the strain PUMC01

used in the macaques model, and to the more than 100 other published SCV strains, representing those isolated during different phases of the SCV evolution as recently defined ***(6)*** with wide geographic distributions around the world (**Fig. 1a**); (b) siSC2 and siSC5 are the two most potent inhibitors for reducing SCV replication in FRhK-4 cells, among a set of active siRNA duplexes selected from 48 siRNA duplexes targeting entire SCV genome ***(29)***; (c) a synergic effect of anti-SCV activity was observed when a combination of siSC2 and siSC5 was applied in the cell culture study, showing the strongest prophylactic and therapeutic effects (**Fig. 1b, c**) among many other combinations with those active siRNA duplexes ***(29)***; (d) the targeted sequences of siSC2 and siSC5 share no homology to the human genome, avoiding potential nonspecific knockdown of patient endogenous genes. In addition, a pair of nonrelated siRNA duplexes, siCONa and siCONb, with no homology to either the human genome or the SARS genome, validated in the cell culture study showing no RNAi activity for SCV inhibition, was chosen as the negative control in the macaque study.

6. Carrier/delivery reagent: TransIT-TKO and polyethyleneimine (PEI) have been reported as carriers for intranasal ***(35)***, intratracheal ***(36)***, and intravenous ***(37)*** deliveries of siRNA into mouse models for treatments of influenza virus and RSV infections. However, these carriers are not feasible for clinical use; PEI, in particular, can induce severe lung inflammation through either intravenous and intratracheal delivery in mice based on our experience and the literature ***(35,37–40)***. We have tested D5W solution ***(41)*** and Infasurf™ solution ***(42)***, which were also applied in animal model deliveries of DNA ***(43)*** and siRNA ***(44)***. Codelivery of pCI-scLuc plasmid with siSC2-5 in D5W solution illustrates a higher level of reporter gene expression and stronger RNAi effect than those in the Infasurf™ solution (**Fig. 1d**).
7. Amount of nucleic acid: We have observed no lung damage with intratracheal delivery of 60 μg of the nucleic acid, providing a safe baseline for siRNA dosing in the respiratory tract of larger mammals.
8. Scoring of pathology in rhesus macaques: Varying degrees of severity of lung damage are scored in microscopic inspection of tissue sections. We adopted a six-grade scoring system (**Fig. 2a–f**): (1) "normal," lung tissue from the control animal without SCV infection; (2) "±", almost normal, slightly broadening of alveolar septa and sparse monocyte infiltration; (3) "+", hemorrhage in septa, elastic fibers of alveolar wall distorted as shown by silver staining; (4) "++", alveolus septa broadening with increasing infiltration of inflammatory cells; (5) "+++", extensive exudation and septa broadening, shrinking of alveoli caused by pressure, restricted fusion of the thick septa, obvious septa hemorrhage, ruptured elastic fiber of alveolar wall, and slight filtration in alveolar cavities; (6) "++++", massive cell filtration and alveoli shrinking, sheets of septa fusion, necrotic lesions at the hemorrhagic septa, and massive cell filtration in alveolar cavities.
9. Features of acute DAD in SCV-infected rhesus macaque lungs: SCV-induced DAD in lower airway was first observed in SARS patients with disease for more than 10 days ***(9)***, while the SCV-infected macaque lungs started developing acute

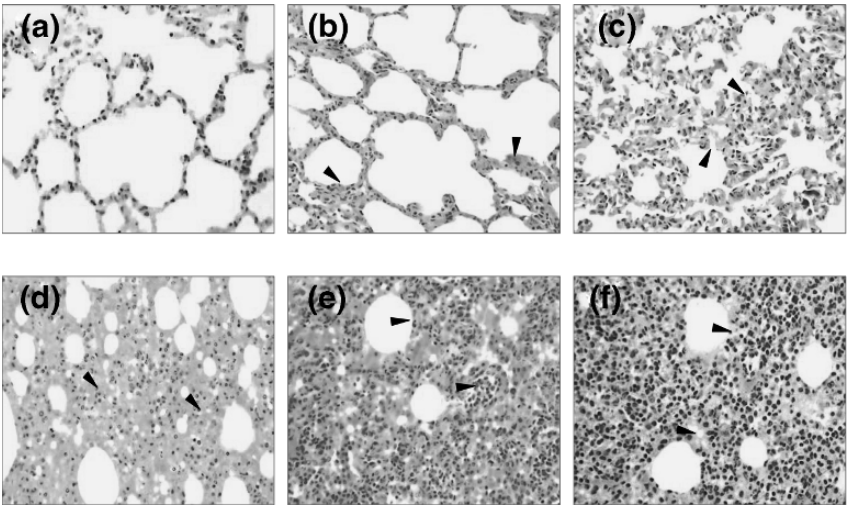

Fig. 2. Severity of lung histopathology in SCV-challenged macaques. All lung histology sections were stained with H&E and magnified X100, and the sample IDs are marked at the top right corner of each image. (a) Normal lung section from macaque #921 without SCV infection (−). (b) Minor inflammation (±) of SCV-infected lung with the prophylactic treatment, from macaque #138. (c) Apparent inflammation (+) of SCV-infected lung with the codelivery treatment, from macaque #077. (d) Early symptom of acute DAD (++) of SCV-infected lung with the postexposure treatment, from macaque #015. (e) Typical symptom of acute DAD (+++) of SCV-infected lung of macaque #212 in the viral infection control group. (f) Severe acute DAD (++++) of SCV-infected lung of macaque #202 in the nonspecific siRNA control group.

DAD at 4 d.p.i. ***(21,23)***. In histopathology and immunohistochemistry microscopic inspection, we found that most of the necropsied lungs had developed acute DAD with various degrees of severity. The typical features of the SCV infection-induced lung (both 7 and 20 d.p.i.) are (a) broken alveolar walls and interstitial edema (**Fig. 3a**); (b) hyaline-membrane formation along the alveoli and pneumocyte desquamation (**Fig. 3b**); (c) damaged alveolus filled with hemorrhage and pneumocytes with nuclear enlargement, prominent nucleolus, and amphophilic granular cytoplasm (**Fig. 3c**); and (**d**) interstitial infiltrates with neutrophils, lymphocytes and macrophages (**Fig. 3d**). Within damaged lung tissues, one can also identify viral-infected pneumocytes, infiltrated neutrophils, lymphocytes, and monocytes that are characteristic of lung inflammation and characterized using keratin (**Fig. 3e**), CD68 (**Fig. 3f**), CD4, CD8, and CD35 immunohistochemical staining (data not shown). These observations are very similar to the lung damage observed in human patients ***(9,10)*** and in a couple of the SARS macaque models ***(21–23)***.

10. Suppression of SARS-like symptoms by siRNA: An effective siRNA will reduce essentially all clinical symptoms described above, showing significant lowering

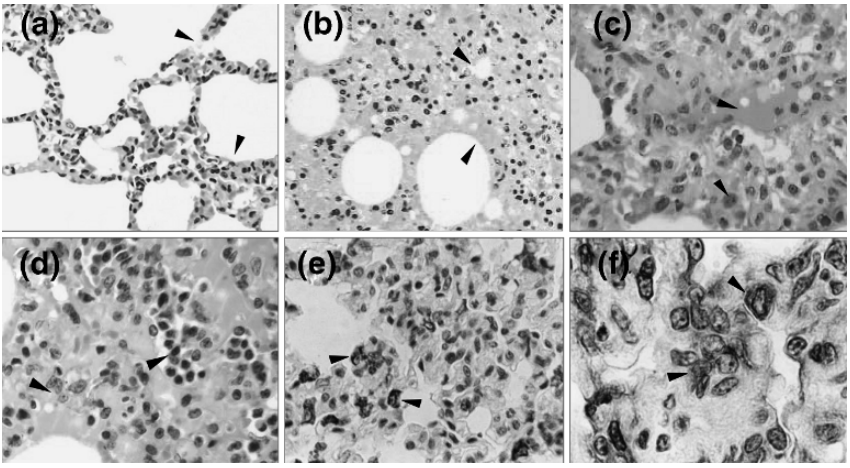

Fig. 3. Histopathological characters of SCV-infected macaque lungs ***(34)***. (a, b) Lung sections were stained with H&E and magnified X150: (a) Section from macaque #214 shows the alveolar walls collapsed and acute diffuse interstitial injury with interstitial edema as arrows indicated at early stage of the disease; (b) section from macaque #015 shows hyaline-membrane formation indicated with arrows along the alveoli and pneumocyte desquamation. (c, d) Lung sections stained with H&E at high-power magnification of X200: (c) Section from macaque #166 shows damaged alveoli were filled with hemorrhage and inflammatory cells indicated by arrows and pneumocytes with nuclear enlargement, prominent nucleolus and amphophilic granular cytoplasm resulting in focal giant-cell formation as arrows indicate; (d) section from macaque #202 shows the inflammatory cells, including neutrophils, lymphocytes, macrophages, and monocytes, were presented in the damaged alveoli. (e) IHC staining of SCV-infected monkey lung section with keratin-specific mAb indicates the epithelium origin pneumocytes pointed to by arrows, X200. (f) IHC staining of SCV-infected monkey lung section with CD68 mAb indicates microphage infiltrates as arrow points, X400.

of pathology scores. Suppression of SCV-induced fever is one of the most obvious and easily detectable siRNA effects in the rhesus macaque model. SCV-specific IgG titer in every blood sample collected at various time points also illustrates an inhibitory effect of siSC2-5 in treated animals (**Fig. 4c**). The SCV-specific IgG levels in IC and NS groups are detected as early as 10 d.p.i., but not in the CD and PE groups. Interestingly, the SCV specific IgG of PL group is detected at 10 d.p.i., suggesting a different mechanism of action for anti-SARS activity. Meanwhile, the SCV-specific IgG levels of all groups are well above detectable level at 19 d.p.i.

11. Inhibition of SCV replication in macaque respiratory tract by siRNA: In addition to acting as an antiviral in the lung, the siRNA shows strong efficacy in the upper respiratory tract. This can be revealed by RT-PCR analysis of oropharyngeal swab samples at 4 d.p.i. (**Fig. 5**).

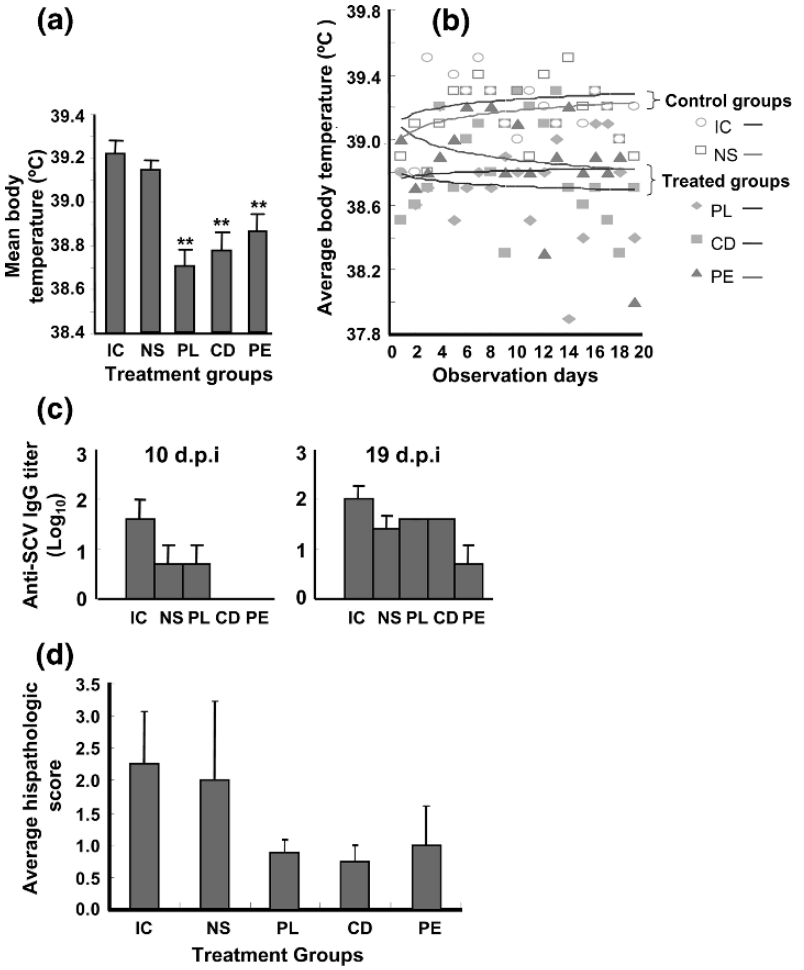

Fig. 4. siSC2-5 relived SARS symptoms ***(34)***. The treatment group abbreviations have been described at the beginning of **Section 4.** (a) Mean body temperature comparison. Mean body temperature represents mean value of average body temperature of each group during the 20-day period. ** indicated the statistical significance compared to IC for t-test, $P < 0.01$, $N = 20$ (days). (b) Distribution of the average body temperatures throughout the 20-day period. The regression analysis was conducted based on the average body temperature of each group on each day. The average body temperature of each group was calculated with $N = 4$ before 7 d.p.i. and $N = 2$ afterward. (c) Anti-SCV antibody was detected in serum samples of IC, NS and PL groups, but not in CD and PE groups, collected at 10 d.p.i. The antibody titers of the IC, NS, and PL groups were increased with detectable titers of CD and PE groups at 19 d.p.i. (d) The average histopathological scores of each group including lung samples collected at both 7 d.p.i and 20 d.p.i. had been compared to the IC group. * indicates *t*-test result of $P < 0.05$, $N = 4$.

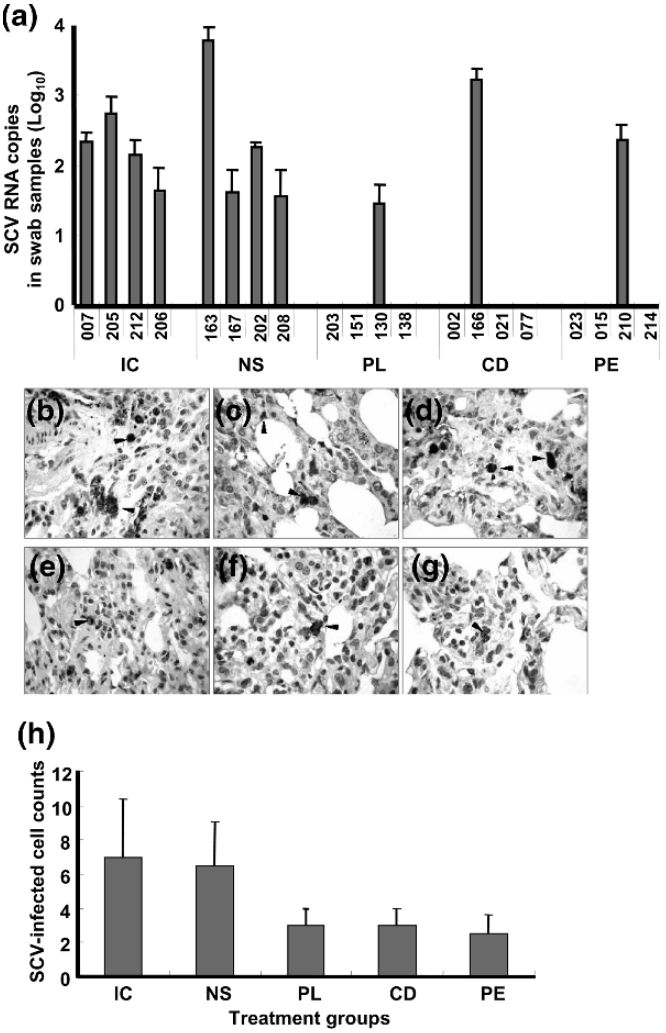

Fig. 5. siSC2-5 inhibits SCV replication ***(34)***. The treatment group abbreviations have been described at the beginning of Section 4. (a) RT-PCR detections of SCV RNA from oropharyngeal swab specimens collected at 4 d.p.i. show positive in all macaques from the control groups, but only 25% of the macaques in three treated groups. (b–g) The SCV-specific antigen was detected in alveoli of deep lungs including various infected cell types at high-power magnification of X200, confirmed by the specific mAb staining. The arrows point to the following: (b) type II pneumocyte (upper arrow) and infected alveolar macrophage; (c) SCV-infected type I pneumocytes; (d) alveolar macrophages; (e–g) scattered infected cells in siSC2-5-treated lungs. (h) Comparison of average SCV infected cell counts of each group with IC group. * indicates *t*-test result of $P < 0.05$, $N = 4$.

12. Prophylactic effects of siRNA: Note that delivering the siSC2-5 prior to SCV infection in PL group using a single dose is able to achieve a comparable inhibitory effect to that of the CD and PE groups. This prophylactic anti-SCV activity resulted in lowered body temperature (**Fig. 4a, b**), milder lung damage (**Fig. 4d**), less viral RNA detected (**Fig. 5a**), and lowered numbers of SCV-infected cells in the lung (**Fig. 5h**), in comparison with the CD and PE treatment groups. This prophylactic efficacy could be a combination of direct degradation of viral RNA by pre-existing intracellular siSC2-5 within the upper airway cells when the viral particle enters, decreasing replication and spread of SCV particles reaching deeper into the lungs, and a cellular antiviral activity induced by siRNA transfection (other than interferon response, ***(45–53)***).

Acknowledgments

This study is supported in part by the Science and Technology Commission, Guangdong Provincial Government, Guangzhou Science and Technology Bureau, Guangzhou Economic & Technological Development District, and China World Trade Corporation (Guangzhou), Top Biotech, Ltd. (Hong Kong), China. We thank Mr. Chun Lu, Mr. Xiaoshun Zhang, and Dr. Decheng Zheng of Top Genomics, Ltd., for their administrative work to coordinate and facilitate the study; Hong Gao, Xinmin Tu, Linlin Bao, Wei Deng, and Binglin Zhang from the Institute of Laboratory Animal Science, Chinese Academy of Medical Sciences & Peking Union Medical College, Beijing, for their technical support during the study; Drs. Walter Tian and Eric Lader of Qiagen for their collaborative efforts; Professor Gu Yingying of the Guangzhou Institute of Respiratory Diseases for her advice on lung pathological analysis; and ONY Inc., Amherst, New York, for providing Infasurf™.

References

1. Fouchier, R. A., Kuiken, T., Schutten, M., et al. (2003). Aetiology: Koch's postulates fulfilled for SARS virus. *Nature* **423**, 240.
2. Kuiken, T., Fouchier, R. A., Schutten, M., et al. (2003). Newly discovered coronavirus as the primary cause of severe acute respiratory syndrome. *Lancet* **362**, 263–270.
3. Ksiazek, T. G., Erdman, D., Goldsmith, C. S., et al. (2003). A novel coronavirus associated with severe acute respiratory syndrome. *N. Engl. J. Med*. **348**, 1953–1966.
4. Peiris, J. S., Lai, S. T., Poon, L. L., et al. (2003). Coronavirus as a possible cause of severe acute respiratory syndrome. *Lancet* **361,** 1319–1325.
5. Guan, Y., Zheng, B. J., He, Y. Q., et al. (2003). Isolation and characterization of viruses related to the SARS coronavirus from animals in Southern China. *Science* **203**, 276–278.

6. Chinese SARS Molecular Epidemiology Consortium (2004). Molecular evolution of the SARS coronavirus during the course of the SARS epidemic in China. *Science* **303**, 1666–1669.
7. Snijder, E. J., Bredenbeek, P. J., Dobbe, J. C., et al. (2003). Unique and conserved features of genome and proteome of SARS-coronavirus, an early split-off from the coronavirus group 2 lineage. *J. Mol. Biol*. **331,** 991–1004.
8. Marra, M. A., Jones, S. J., Astell, C. R., et al. (2003). The genome sequence of the SARS-associated coronavirus. *Science* **300**, 1399–1404.
9. Nicholls, J. M., Poon, L. L., Lee, K. C., et al. (2003). Lung pathology of fatal severe acute respiratory syndrome. *Lancet* **361**, 1773–1778.
10. Peiris, J. S., Chu, C. M., Cheng, V. C., et al. (HKU/UCH SARS Study Group) (2003). Clinical progression and viral load in a community outbreak of coronavirus-associated SARS pneumonia: A prospective study. *Lancet* **361,** 1767–1772.
11. Mashall, E., and Enserink, M. (2004). Caution urged on SARS vaccines. *Science* **303**, 944–946.
12. Bisht, H., Roberts, A., Vogel, L., et al. (2004). Severe acute respiratory syndrome coronavirus spike protein expressed by attenuated vaccinia virus protectively immunizes mice. *Proc. Natl. Acad. Sci. USA* **101**, 6641–6646.
13. Bukreyev, A., Lamirande, E. W., Buchholz, U. J., et al. (2004). Mucosal immunization of African green monkeys (*Cercopithecus aethiops*) with an attenuated parainfluenza virus expressing the SARS coronavirus spike protein for the prevention of SARS. *Lancet* **363**, 2122–2127.
14. Yang, Z. Y., Kong, W. P., Huang, Y., et al. (2004). A DNA vaccine induces SARS coronavirus neutralization and protective immunity in mice. *Nature* **428,** 561–564.
15. Hogan, R. J., Gao, G., Rowe, T., et al. (2004). Resolution of primary severe acute respiratory syndrome-associated coronavirus infection requires Stat1. *J. Virol*. **78**, 11416–11421.
16. Zhong, N. S., Zheng, B. J., Li, Y. M., et al. (2003). Epidemiology and cause of severe acute respiratory syndrome (SARS) in Guangdong, People's Republic of China, in February 2003. *Lancet* **362**, 1353–1358.
17. Subbarao, K., McAuliffe, J., Vogel, L., et al. (2004). Prior infection and passive transfer of neutralizing antibody prevent replication of severe acute respiratory syndrome coronavirus in the respiratory tract of mice. *J. Virol*. **78**, 3572–3577.
18. Hensley, L. E., Fritz, L. E., Jahrling, P. B., Karp, C. L., Huggins, J. W., and Geisbert, T. W. (2004). Interferon-β 1a and SARS coronavirus replication. *Emerg. Infect. Dis.* **10**, 317–319.
19. Spiegel, M., Pichlmair, A., Muhlberger, E., Haller, O., and Weber, F. (2004). The antiviral effect of interferon-β against SARS-coronavirus is not mediated by MxA protein. *J. Clin. Virol*. **30**, 211–213.
20. Sainz, B., Jr., Mossel, E. C., Peters, C. J., and Garry, R. F. (2004). Interferon-beta and interferon-gamma synergistically inhibit the replication of severe acute respiratory syndrome-associated coronavirus (SARS-CoV). *Virology* **329**, 11–17.

21. Haagmans, B. L., Kuiken, T., Martina, B. E., et al. (2004). Pegylated interferon-α protects type 1 pneumocytes against SARS coronavirus infection in macaques. *Nat. Med*. **10**, 290–293.
22. Rowe, T., Gao, G., Hogan, R. J., et al. (2004). Macaque model for severe acute respiratory syndrome. *J. Virol*. **78**, 11401–11404.
23. Qin, C., et al. (2004). Histological changes in SARS-CoV infected rhesus monkeys. *Proc. Chinese Assoc. Experimental Animal Res*., 38–45.
24. Wei, Q., et al. (2004). Virologic and serologic detection of SARS-CaV in infected rhesus monkey. *Proc. Chinese Assoc. Experimental Animal Res*., 46–48.
25. Chen, Z., Zhang, L., Qin, C., et al. (2005). Recombinant modified vaccinia virus Ankara expressing the spike glycoprotein of severe acute respiratory syndrome coronavirus induces protective neutralizing antibodies primarily targeting the receptor binding region. *J. Virol*. **79,** 2678–2688.
26. Qin, C., Wang, J., Wei, Q., et al. (2005). An animal model of SARS produced by infection of *Macaca mulatta* with SARS coronavirus. *J. Pathol.* **206,** 251–259.
27. Haasnoot, P. C., Cupac, D., and Berkhout, B. (2003). Inhibition of virus replication by RNA interference. *J. Biomed. Sci*. **10**, 607–616.
28. Bitko, V., and Barik, S. (2001). Phenotypic silencing of cytoplasmic genes using sequence-specific double-stranded short interfering RNA and its application in the reverse genetics of wild type negative-strand RNA viruses. *BMC Microbiol*. **1,** 34.
29. Zheng, B. J., Guan, Y., Tang, Q., et al. (2004). Prophylactic and therapeutic effects of small interfering RNA targeting SARS-coronavirus. *Antivir. Ther*. **9**, 365–374.
30. Elmen, J., Wahlestedt, C., Brytting, M., Wahren, B., and Ljungberg, K. (2004). SARS virus inhibited by siRNA. *Preclinica* **2**, 135–142.
31. Zhang, Y., Li, T., Fu, L., et al. (2004). Silencing SARS-CoV protein expression in cultured cells by RNA interference. *FEBS Lett*. **560,** 141–146.
32. Zhang, R., Guo, Z., Lu, J., et al. (2003). Inhibiting severe acute respiratory syndrome-associated coronavirus by small interfering RNA. *Chin. Med. J. (Engl.)* **116**, 1262–1264.
33. Wang, Z., Ren, L., Zhao, X., et al. (2004). Inhibition of severe acute respiratory syndrome virus replication by small interfering RNAs in mammalian cells. *J. Virol*. **78**, 7523–7527.
34. Li, B. J., Tang, Q., Cheng, D., et al. (2005). Using siRNA in prophylactic and therapeutic regimens against SARS coronavirus in Rhesus macaque. *Nat. Med*. **11,** 944–951.
35. Bitko, V., Musiyenko, A., Shulyayeva, O., and Barik, S. (2005). Inhibition of respiratory viruses by nasally administered siRNA. *Nat. Med*. **11**, 50–55.
36. Tompkins, S. M., Lo, C. Y., Tumpey, T. M., and Epstein, S. L. (2004). Protection against lethal influenza virus challenge by RNA interference *in vivo*. *Proc. Natl. Acad. Sci. USA* **101**, 8682–8686.
37. Ge, Q., Filip, L., Bai, A., Nguyen, T., Eisen, H. N., and Chen, J. (2004). Inhibition of influenza virus production in virus-infected mice by RNA interference. *Proc. Natl. Acad. Sci. USA* **101**, 8676–8681.

38. Trubetskoy, V. S., Wong, S. C., Subbotin, V., et al. (2003). Recharging cationic DNA complexes with highly charged polyanions for *in vitro* and *in vivo* gene delivery. *Gene Ther.* **10**, 261–271.
39. Boeckle, S., von Gersdorff, K., van der Piepen, S., Culmsee, C., Wagner, E., and Ogris, M. (2004). Purification of polyethylenimine polyplexes highlights the role of free polycations in gene transfer. *J. Gene Med.* **6**, 1102–1111.
40. Delepine, P., Guillaume, C., Montier, T., et al. (2003). Biodistribution study of phosphonolipids: A class of non-viral vectors efficient in mice lung-directed gene transfer. *J. Gene Med*. **5,** 600–608.
41. Ghanayem, N. S., Yee, L., Nelson, T., et al. (2001). Stability of dopamine and epinephrine solutions up to 84 hours. *Pediatr. Crit. Care Med*. **2,** 315–317.
42. Thomas, N. J., Hollenbeak, C. S., Lucking, S. E., and Willson, D. F. (2005). Cost-effectiveness of exogenous surfactant therapy in pediatric patients with acute hypoxemic respiratory failure. *Pediatr. Crit. Care Med*. **6,** 160–165.
43. Ennist, D., et al. (2000). Method of achieving persistent transgene expression. U.S. patent application 20030148975, PCT/EP00/13297.
44. Massaro, D., Massaro, G. D., and Clerch, L. B. (2004). Noninvasive delivery of small inhibitory RNA and other reagents to pulmonary alveoli in mice. *Am. J. Physiol. Lung Cell Mol. Physiol*. **287,** 1066–1070.
45. Sledz, C. A., Holko, M., de Veer, M. J., Silverman, R. H., and Williams, B. R. (2003). Activation of the interferon system by short-interfering RNAs. *Nat. Cell Biol*. **5**, 834–839.
46. Kariko, K., Bhuyan, P., Capodici, J., and Weissman, D. (2004). Small interfering RNAs mediate sequence-independent gene suppression and induce immune activation by signaling through Toll-like receptor 3. *J. Immunol*. **172**, 6545–6549.
47. Heidel, J. D., Hu, S., Liu, X. F., Triche, T. J., and Davis, M. E. (2004). Lack of interferon response in animals to naked siRNAs. *Nat. Biotechnol*. **22**, 1579–1582.
48. Judge, A. D., Sood, V., Shaw, J. R., Fang, D., McClintock, K., and MacLachlan, I. (2005). Sequence-dependent stimulation of the mammalian innate immune response by synthetic siRNA. *Nat. Biotechnol.* **23,** 457–562.
49. Hornung, V., Guenthner-Biller, M., Bourquin, C., et al. (2005). Sequence-specific potent induction of IFN-α by short interfering RNA in plasmacytoid dendritic cells through TLR7. *Nat. Med*. **11,** 263–270.
50. Bonnard, E., Mazarguil, H., and Zajac, J. M. (2002). Peptide nucleic acids targeted to the mouse proNPFF(A) reveal an endogenous opioid tonus. *Peptides* **23**, 1107–1113.
51. Semizarov, D., Frost, L., Sarthy, A., Kroeger, P., Halbert, D. N., and Fesik, S. W. (2003). Specificity of short interfering RNA determined through gene expression signatures. *Proc. Natl. Acad. Sci. USA* **100**, 6347–6352.
52. Chi, J. T., Chang, H. Y., Wang, N. N., Chang, D. S., Dunphy, N., and Brown, P. O. (2003). Genomewide view of gene silencing by small interfering RNAs. *Proc. Natl. Acad. Sci. USA* **100**, 6364–6369.

53. Jackson, A. L., Bartz, S. R., Schelter, J., et al. (2003). Expression profiling reveals off-target gene regulation by RNAi. *Nat. Biotechnol*. **21**, 635–637.
54. Ware, L. B., and Matthay, M. A. (2000). The acute respiratory distress syndrome. *N. Engl. J. Med*. **342**, 1334–1349.
55. Yuen, K. Y., Chan, P. K., Peiris, M., et al. (1998). Clinical features and rapid viral diagnosis of human disease associated with avian influenza A H5N1 virus. *Lancet* **351**, 467–471.
56. Huang, K. J., Su, I. J., Theron, M., et al. (2005). An interferon-gamma-related cytokine storm in SARS patients. *J. Med. Virol*. **75,** 185–194.
57. Cinatl, J., Morgenstern, B., Bauer, G., Chandra, P., Rabenau, H., and Doerr, H. W. (2003). Treatment of SARS with human interferons. *Lancet* **362**, 293–294.